International Journal of Solids and Structures 51 (2014) 4052–4067

Contents lists available at ScienceDirect

International Journal of Solids and Structures

journal homepage: www.elsevier.com/locate/ijsolstr

Buckling and post-buckling of gradient and nonlocal plasticity columns experiencing softening

Vincent Picandet *, Noël Challamel, Sovannara Hin

Université de Bretagne Sud, EA 4250, LIMATB, F-56100 Lorient, France

ARTICLE INFO

Article history:
Received 6 September 2013
Received in revised form 14 April 2014
Available online 12 August 2014

Keywords:
Buckling
Elastoplasticity
Gradient plasticity
Variational principle
Softening
Structure

ABSTRACT

The buckling and the post-buckling behaviors of a perfect axially loaded column are analytically investigated through a global bilinear moment–curvature elastoplastic constitutive law. Three plasticity cases are studied, namely the linear hardening plasticity law, the perfect elastoplastic case and the softening case. The applications of such a study can be found in various structural engineering problems, including reinforced concrete, steel, timber or composite structures. It is analytically shown that for all kinds of elastoplastic behaviors, the plasticity phenomena lead to a global softening branch in the load–deflection diagram. The propagation of the plasticity zone during the post-buckling process is analytically characterized in case of linear hardening or softening plasticity laws. However, it is shown that the unphysical elastic unloading solution necessarily occurs in presence of local softening moment–curvature constitutive law. A nonlocal plasticity moment–curvature softening law is then used to control the localization branch in the post-buckling stage. This nonlocal plasticity law includes the explicit and the implicit gradient plasticity law. Higher-order plasticity boundary conditions are derived from an extended variational principle. Some parametric studies finally illustrate the main findings of this paper, including the plasticity modulus effect on the post-buckling behavior of these plasticity structural systems.

1. Introduction

This paper is focused on the buckling and post-buckling behavior of elastoplastic columns with hardening or softening moment–curvature constitutive law. Softening is understood in this study as a decrease of the stress variable (or the bending moment variable at the beam scale) for an increase of the strain variable (or the curvature at the beam scale). This phenomenon typically arises when the material loses its strength during a degrading loading process. A lot of engineering applications are concerned by such kind of elastoplastic moment–curvature models, which may be used for characterizing the ultimate behavior of inelastic structural elements.

Softening moment–curvature laws were probably first introduced for modeling cracking phenomena in reinforced concrete beams (Wood, 1968). Such engineering bending moment–curvature models can be useful for the fundamental understanding of the collapse of structural members. For instance, these beam models can be used to compute the global behavior of structural members composed of quasi-brittle materials experiencing some material softening phenomenon beyond a critical threshold (reinforced concrete members, timber beams, composite members... see for instance Wood (1968), Bažant (1976), Jirásek and Bažant (2002), Bažant and Cedolin (2003), Casandjian et al. (2013) and Hellesland et al. (2013)). On the other hand, geometrical softening may also be modeled in a simplified unidimensional approach, with such a bending-curvature constitutive law. This geometrically nonlinear softening phenomenon is associated in this case with the local buckling phenomenon of thin walled structured. For instance, the plastic buckling of tubes in bending, coupled with the so-called ovalization phenomenon, can be modeled with such a hardening–softening moment curvature relationship (Calladine, 1982; Kyriakides and Ju, 1992; Yu et al., 1993; Reid et al., 1998; Kyriakides et al., 2008; Poonaya et al., 2009). The bending response of steel thin-walled members can also experience a softening stage induced by the local buckling phenomenon (Mazzolani and Gioncu, 2002). The localization process in these hardening–softening structural members has been already investigated in details for bending problems, but the coupling between softening and second-order geometrical effects at the beam scale has not been investigated in details in the literature, to the author's knowledge, at least for plasticity structural systems.

* Corresponding author.
E-mail addresses: vincent.picandet@univ-ubs.fr (V. Picandet), noel.challamel@univ-ubs.fr (N. Challamel), sovannara.hin@univ-ubs.fr (S. Hin).

http://dx.doi.org/10.1016/j.ijsolstr.2014.07.020
0020-7683/

To allow for analytical calculations, a linear hardening/softening modulus is considered in this paper for the bending moment curvature constitutive law. This is in concordance with the model of Wood (1968) in case of linear softening applied to reinforced concrete members. Vaz and Patel (2007) also studied a bilinear bending moment–curvature law for flexible pipes applications, with a plasticity hardening branch. Linear hardening moment–curvature can be also deduced at the beam cross section level from local stress–strain relationship, as shown for instance by Casandjian et al. (2013).

The bending behavior of such elastoplastic systems is well studied in the literature. In particular, it is shown since the seminal work of Wood (1968) that a local elastoplastic softening moment–curvature constitutive law leads to an unphysical elastic unloading solution. It is now well accepted that a nonlocal model including some additional length scales, has to be considered for softening media (and also for softening beams). For instance, Pijaudier-Cabot and Bažant (1987) developed a nonlocal Continuum Damage Mechanics model to control the localization process in the softening range. A lot of numerical results have been performed for such nonlocal structural elements (see for instance Jirásek and Bažant (2002)) but very few analytical results are available for bending or buckling of nonlocal inelastic softening elements. Such reference solutions are useful for a better understanding of the deep scenario of the localization process induced by the softening part of the constitutive law.

Nonlocal plasticity can be implemented in a gradient-based or integral-based version. The pioneer solutions for the gradient plasticity models were probably first elaborated by Mühlhaus and Aifantis (1991) and de Borst and Mühlhaus (1992) for a homogeneous bar under uniaxial loading, exhibiting some specific periodic localized solutions. Later, Challamel (2003) developed a gradient plasticity moment–curvature model, and obtained some similar localization solutions in case of uniform bending, controlled by the beam length scales. Challamel et al. (2008) generalized these solutions for the non-uniform bending of gradient plasticity or nonlocal-based softening beams. Challamel et al. (2010) also shown the link between gradient plasticity and nonlocal integral-based plasticity, in an archetypal elastoplastic hardening–softening beam. Polizzotto (2007) obtained some other kinds of solutions for a gradient plasticity model with hardening. The paper of Peerlings (2007) should be also mentioned for a theoretical analysis of a gradient plasticity beam under uniform bending. More recently, Jirásek et al. (2013) obtained some new solutions for the axial behavior of non-homogeneous gradient plasticity softening bars.

If the bending behavior of nonlocal elastoplastic beam systems has been now well investigated, the stability behavior of such enriched elastoplastic systems is probably less studied. This paper aims at developing a rational analysis of the buckling and post-buckling behavior of some straight columns, modeled by an elastoplastic hardening or softening moment–curvature model. A typical application concerned by this model is the stability behavior of reinforced concrete column. The coupling between material instability (associated with the local softening behavior) and structural stability has not been exhaustively explored for such structural problems. It is worth mentioning that the buckling and post-buckling behavior of a column with a bilinear moment–curvature law (with positive hardening) has been studied by Vaz and Patel (2007) in a geometrically exact framework. More recently, Challamel and Hellesland (2013) investigated the buckling and post-buckling behavior of nonlocal Continuum Damage Mechanics columns, and used asymptotic methods to highlight the specific imperfection sensitive phenomenon.

In this paper, the buckling behavior of a clamped column with a free end (cantilever column) is investigated. The column is modeled by an elastoplastic moment–curvature law with or without gradient terms. The gradient terms have been introduced for regularizing the softening problem which would have been not well-posed without this enriched constitutive law. The column is assumed to be homogeneous with a length L and with a constant cross section. An axially centered load P acts at the top of the perfect column (no initial imperfection for this problem). The deflection of the column with respect to its fundamental state is denoted by $w(x)$ (see Fig. 1)

2. Differential equations

2.1. Governing equation

We first start from the weak form of the equilibrium equations via the principle of virtual work:

$$\int_0^L M\delta w'' - Pw'\delta w' = 0 \tag{1}$$

leading to the direct equilibrium equations:

$$M'' + Pw'' = 0 \tag{2}$$

It is assumed that the behavior of the column is ruled by an elastoplastic moment–curvature relationship with a linear hardening (or linear softening), see Fig. 2. In case of softening, the gradient plasticity terms are added for restoring the well-posedness of the evolution problem (if the regularized problem still remains well-posed).

The constitutive law at the cross section level may be written from the bending moment–elastic curvature relationship:

$$M = EI(w'' - \chi_p) \tag{3}$$

where the curvature χ is related to the second-order derivative of the deflection $\chi = w''$, χ_p is the plastic curvature, and EI is the elastic bending stiffness.

The loading function combines a gradient plasticity model with a nonlocal integral-based plasticity model and is given by the following differential equation:

$$M - l_c^2 M'' = M_p + k_p\left(\chi_p + a^2\chi_p''\right) \tag{4}$$

This loading function depends on two length scales, namely l_c and a. The gradient plasticity model is found for the specific case $l_c = 0$. M_p is the plastic moment; k_p positive corresponds to a positive hardening behavior, whereas a negative value of k_p corresponds to a softening behavior. The perfect elastoplastic behavior is associated with a vanishing plastic modulus $k_p = 0$. Such kind of nonlocal plasticity laws has been successfully used by Challamel et al. (2008) or Challamel et al. (2010) for accurate computation of the bending collapse of elastoplastic beams. This model has been shown to be cast in a so-called micromorphic plasticity framework (see Forest (2009) or Challamel et al. (2010)). It is known that nonlocal plasticity can accurately control the post-failure process in softening three-dimensional media (Jirásek and Bažant, 2002). It has been shown that the nonlocal plastic loading function considered in Eq. (4) can be used for softening moment–curvature, in order to avoid localization in infinitely small areas along the beam (Challamel, 2008). Such kind of implicit gradient dependent yield condition is also generally considered by Aifantis (2011) for other applications at the material scale.

2.2. Elastic buckling and elastoplastic post-buckling

For sufficiently small curvatures after the buckling of the elastoplastic column, the column remains in its elastic phase, meaning

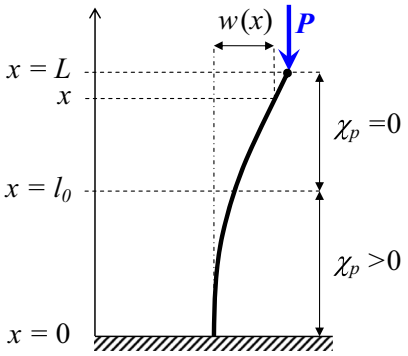

Fig. 1. Buckling of the cantilever column due to axially centered load, P.

that the classical differential equations of the buckling problem can be considered:

$$|M(0)| \leqslant M_p \Rightarrow EIw^{(4)} + Pw'' = 0 \tag{5}$$

with the following boundary conditions:

$$w(0) = 0; \quad w'(0) = 0; \quad EIw''(L) = 0 \text{ and } EIw'''(L) + Pw'(L) = 0 \tag{6}$$

The buckling load, $P = \pi^2 EI/4L^2$, is constant during the initial elastic post-buckling range for sufficiently small curvatures (as far as the linearized theory is considered). Note that the load would not have been constant in a geometrically exact framework even in the elasticity range, see also Vaz and Patel (2007) for a column with bilinear moment–curvature analyzed in a geometrically exact framework. In this paper, a small rotation theory is used, leading to a more tractable linear boundary value problem. The elastoplastic process has then to be considered for sufficiently large curvatures, as detailed by:

$$\frac{\pi^2}{4}\frac{EI}{L^2}w(L) \geqslant M_p \tag{7}$$

In the elastoplastic range, by considering the equilibrium equations, see Eq. (2), the local constitutive law, see Eq. (3), and by introducing the non-locality criteria, see Eq. (4), a system of coupled differential equations with two unknown fields (w, χ_p) is obtained:

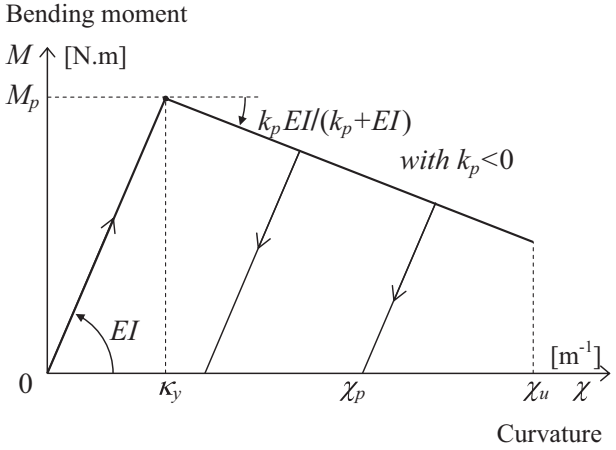

Fig. 2. Elastoplastic bending moment–curvature law with a linear hardening ($k_p > 0$) or softening ($k_p < 0$) behavior beyond the maximum elastic curvature κ_y. The representation is based on the softening case, i.e. $k_p < 0$.

$$\begin{cases} EI\left(w^{(4)} - \chi_p''\right) + Pw'' = 0 \\ EI\left(w'' - \chi_p\right) = M_p + k_p\left(\chi_p + a^2\chi_p''\right) + l_c^2 M'' \end{cases} \tag{8}$$

2.3. Dimensionless parameters

Thereafter, the following dimensionless parameters, normalized with respect to the physical characteristics of the column, i.e.: L, E and I are introduced to correspond to: longitudinal coordinate, x^*; limit of the plasticized zone, l_0^*; characteristic lengths, α and λ_c; deflection, w^*; applied load, β; plastic curvature, χ_p^*; plastic bending modulus, k_p^*; and the dimensionless yield elastic curvature, κ_Y^*, associated to the plasticity moment, see Eq. (4) and Fig. 2.

$$\begin{aligned} &x^* = \frac{x}{L}; \quad l_0^* = \frac{l_0}{L}; \quad \alpha = \frac{a}{L}; \quad \lambda_c = \frac{l_c}{L}; \quad w^* = \frac{w}{L} \\ &\beta = \frac{PL^2}{EI}; \quad \chi_p^* = \chi_p L; \quad k_p^* = \frac{k_p}{EI}; \quad \kappa_Y^* = \kappa_Y L = \frac{M_p}{EI}L \end{aligned} \tag{9}$$

In this work, all parameters used and their associated dimensionless parameters can be found in the provided nomenclature. It should be noted that the derivatives of all dimensionless parameters, annotated with prime, are thereafter considered with respect to the dimensionless coordinate, x^*, (i.e. $\partial/\partial x^*$). If the derivatives of the dimensionless deflection are considered, the Eq. (8) can be re-written as follow:

$$\begin{cases} w^{*(4)} - \chi_p^{*''} = -\beta w^{*''} \\ w^{*''} - \chi_p^* = \kappa_Y^* + k_p^*\left(\chi_p^* + \alpha^2\chi_p^{*''}\right) - \lambda_c^2\beta w^{*''} \end{cases} \tag{10}$$

2.4. Differential equation of plastic curvature

The second equation of the system in Eq. (10) gives the second order derivative of the deflection with respect to the plastic curvature and its derivatives.

$$w^{*''} = \frac{k_p^*\alpha^2\chi_p^{*''} + \left(1 + k_p^*\right)\chi_p^* + \kappa_Y^*}{\left(1 + \lambda_c^2\beta\right)} \tag{11}$$

By introducing this relationship in the loading function, the second-order derivative of the deflection can be directly expressed by the plastic curvatures and its derivatives as a fourth-order linear differential equation for the plastic curvature:

$$\alpha^2 k_p^*\chi_p^{*(4)} + \left(k_p^* - \lambda_c^2\beta + \alpha^2\beta k_p^*\right)\chi_p^{*''} + \beta\left(1 + k_p^*\right)\chi_p^* = -\beta\kappa_Y^* \tag{12}$$

3. Resolution – perfect plasticity and hardening

In both cases, perfect plasticity or positive hardening plasticity, the nonlocal plasticity law is not required, at least for deriving a meaningful physical and well-posed solution. Since the plastic bending modulus is assumed to be positive in this part, i.e. $k_p \geqslant 0$, the non-locality parameters introduced in Eq. (4) are assumed to vanish, i.e. $a = 0$ and $l_c = 0$. Of course, nonlocal plasticity can be also introduced even in case of positive hardening, to capture for instance some specific scale effects. But one can say, that these effects are less sensitive for positive hardening compared to the solution of the softening case.

3.1. Perfect elastoplastic problem, ($k_p = 0$)

The border case is the perfect elastoplastic problem without hardening. This problem has been also treated by Challamel (2009) who also combined a lateral load with the axial buckling

load. In such case, the length of the plasticity zone is vanishing, the column behaves elastically, with a moment at the clamped section which is equal to the plastic moment. The perfect elastoplastic evolution problem is then obtained from the "elastic" differential equation.

$$w^{*(4)} + \beta w^{*''} = 0 \tag{13}$$

From this fourth-order differential equation, the general solution of the dimensionless deflection, $w^*(x^*)$ depends on four (A_1, A_2, A_3, A_4):

$$w^*(x^*) = A_1 + A_2 x^* + A_3 \cos\left(x^*\sqrt{\beta}\right) + A_4 \sin\left(x^*\sqrt{\beta}\right) \tag{14}$$

The four boundary conditions of the clamped-free column studied in this paper are:

$$w^*(0) = 0, \quad w^{*'}(0) = \kappa_Y^*, \quad w^{*''}(1) = 0, \text{ and } w^{*'''}(1) + \beta w^{*'}(1) = 0 \tag{15}$$

The identification of the four parameters leads to the elastoplastic solution which is equivalent to introducing a zero-length plasticity hinge as usually performed in limit analysis design:

$$w^*(x^*) = \frac{\kappa_Y^*}{\beta} - \frac{\kappa_Y^*}{\beta}\cos\left(x^*\sqrt{\beta}\right) + \frac{\kappa_Y^*}{\beta\tan\sqrt{\beta}}\sin\left(x^*\sqrt{\beta}\right) \tag{16}$$

If the dimensionless tip deflection, δ^*, is higher than the one obtained at the limit of elasticity, δ_e^*, the corresponding dimensionless deflection of the free end of the column, $\delta^* = w^*(1)$, can be reduced to the following basic relationship, plotted as a reference solution in all tip deflection–load diagrams in this study.

$$\text{if } \delta^* \geqslant \delta_e^* = \frac{4\kappa_Y^*}{\pi^2} \Rightarrow \beta = \frac{\kappa_Y^*}{\delta^*} \tag{17}$$

3.2. Positive hardening with a local constitutive law ($k_p > 0$)

3.2.1. General equation of the deflection

Since the nonlocal length scales are vanishing for the "local" hardening law, i.e. $\alpha = 0$ and $\lambda_c = 0$, the fourth-order differential equation for the plastic curvature given by Eq. (12) is reduced to a second-order linear differential equation.

$$\chi_p^{*''} + \beta\left(\frac{1}{k_p^*} + 1\right)\chi_p^* = -\frac{\beta}{k_p^*}\kappa_Y^* \tag{18}$$

The columns can be split in two parts, see Fig. 1. The first one, from the clamped end to the elastoplastic boundary $x = l_0$, i.e. $x \in [0, l_0]$, is assumed to be in the plasticity range, i.e. $\chi_p \geqslant 0$, while the other part, from l_0 to the free end, i.e. $x \in [l_0, L]$, remains elastic i.e. $\chi_p = 0$.

Since $k_p \geqslant 0$, the dimensionless plastic curvature can be expressed in trigonometric format depending on two constants B_3 and B_4 as follow:

$$\chi_p^* = B_3\cos\left(x^*\sqrt{\rho^+}\right) + B_4\sin\left(x^*\sqrt{\rho^+}\right) - \frac{\kappa_Y^*}{1 + k_p^*} \tag{19}$$

with, (as reminded in the nomenclature):

$$\rho^+ = \beta\left(\frac{1}{k_p^*} + 1\right) \tag{20}$$

If $x \in [0, l_0[$, χ_p^* and w^* are related by Eq. (11) with $\lambda_c = 0$ and $\alpha = 0$. The dimensionless deflection named as $w^{-*}(x^*)$ in the first part of the column where $\chi_p > 0$, see Fig. 1, depends then on four constant parameters: B_1, B_2, B_3, B_4 as follow:

$$w^{*-} = B_1 + B_2 x^* - \frac{k_p^*}{\beta}\left[B_3\cos\left(x^*\sqrt{\rho^+}\right) + B_4\sin\left(x^*\sqrt{\rho^+}\right)\right] \tag{21}$$

Along the upper part of the column, the bending behavior remains in the elastic range, i.e. $\chi_p = 0$ for $x \in [l_0, L]$. The dimensionless deflection denoted by $w^{*+}(x)$ in this elastic zone is deduced from the differential equation given by Eq. (13), and depends on four constant parameters: C_1, C_2, C_3, C_4 as follow:

$$w^{*+} = C_1 + C_2 x^* + C_3\cos\left(x^*\sqrt{\beta}\right) + C_4\sin\left(x^*\sqrt{\beta}\right) \tag{22}$$

3.2.2. Boundary conditions

To solve the deflections of the column in both parts, the nine following boundary conditions are needed to determine the nine unknown parameters used in Eq. (21) and Eq. (22): B_1, B_2, B_3, B_4, C_1, C_2, C_3, C_4 and l_0.

The clamped conditions at the bottom of the column are characterized by the absence of deflection, Eq. (23-a), and the absence of rotation, Eq. (23-b):

$$w^{*-}(0) = 0; \tag{23-a}$$

$$w^{*-'}(0) = 0; \tag{23-b}$$

The continuity conditions at the elastoplastic interface ($x = l_0$), between the plasticity and the elastic parts of the column, are expressed by the vanishing of the plastic curvature at this transition point, Eq. (24-a), the continuity of the deflection, Eq. (24-b), and of its first and second order derivative, Eqs. (24-c) and (24-d) (i.e. the continuity of rotation and of bending moment), and the continuity of the shear force, Eq. (24-e):

$$\chi_p^*(l_0^*) = 0 \tag{24-a}$$

$$w^{*-}(l_0^*) = w^{*+}(l_0^*) \tag{24-b}$$

$$w^{*-'}(l_0^*) = w^{*+'}(l_0^*) \tag{24-c}$$

$$w^{*-''}(l_0^*) = w^{*+''}(l_0^*) \tag{24-d}$$

$$w^{*-'''}(l_0^*) - \chi_P^{*'}(l_0^*) + \beta w^{*-'}(l_0^*) = w^{*+'''}(l_0^*) + \beta w^{*+'}(l_0^*) \tag{24-e}$$

The free end boundary conditions at the top of the column, are associated with the vanishing of both the bending moment, Eq. (25-a), and additional shear force, Eq. (25-b), i.e. the static equilibrium involves the shear force is equal to $-Pw'(1)$.

$$w^{*+''}(1) = 0 \tag{25-a}$$

$$w^{*+'''}(1) + \beta w^{*+'}(1) = 0 \tag{25-b}$$

3.2.3. Propagation of the plasticity zone, l_0

The boundary conditions in Eqs. (23-b), (24-e) and (25-b) lead to the following simplification: $B_2 = B_4 = C_2 = 0$. The other boundary conditions, lead to the following propagation law of the plasticity zone:

$$\sqrt{\frac{k_p^*}{1 + k_p^*}}\tan\left[\sqrt{\beta}(1 - l_0^*)\right]\tan\left(l_0^*\sqrt{\rho^+}\right) = 1 \tag{26}$$

It is worth mentioning that the relationship between l_0^* (or l_0/L ratio) and β does not depend on the yield elastic curvature, (i.e. independent of κ_Y). It can be checked that the characteristic elastic point ($l_0^* = 0; \beta = \pi^2/4$) is solution of Eq. (26) since:

$$l_0^* \to 0 \Rightarrow \left(\sqrt{\frac{1}{k_p^*} + 1}\right)\cos\left[\sqrt{\beta}(1 - l_0^*)\right]\cos\left(l_0^*\sqrt{\rho^+}\right) \to 0 \Rightarrow \beta \to \frac{\pi^2}{4} \tag{27}$$

The post-buckling elastoplastic process starts at the elastic buckling load, where the length of the plasticity zone is initially vanishing and then, the plasticity zone grows during the hardening plastic process.

The function $\beta = f(l_0^*)$ deduced from Eq. (26) presents some discontinuities. Since we limit our study to the first buckling mode, the first discontinuity is observed when $\sqrt{\rho^+}l_0^* \to \pi/2$. If $l_0^* \in]0; \pi/2\sqrt{\rho^+}[$, the function $\beta = f(l_0^*)$ finds a unique solution for β that ranges within the interval $[0; \pi^2/4]$. This unique solution can be accurately computed using numerical methods, such as secant methods as used in this study.

It should be noted that the plasticity process starts when $\beta = \pi^2/4$ and may propagate along the whole length L when $l_0 \to L$. In such case, Eq. (26) leads to:

$$l_0^* \to 1 \Rightarrow \tan\left(\frac{\pi}{2} - \sqrt{\rho^+}\right) \to 0 \Rightarrow \beta \to \frac{\pi^2}{4}\frac{k_p^*}{1+k_p^*} = \beta_f \tag{28}$$

The propagation of the plasticity zone ends when l_0 reaches L, i.e. when β reaches the minimum load capacity of the column remaining at the end of the post buckling path, i.e. beyond the elastic point, β decreases and tends toward the final post-buckling load, β_f. Since l_0 cannot be greater than L, β_f is the minimum bearing load at the end of the post buckling path. It is worth to note that β_f corresponds to the tangent modulus buckling load as introduced by Engesser (see Bažant and Cedolin (2003)). In order to compare the propagation laws according to k_p^* within the interval $\beta \in [\beta_f; \pi^2/4]$ a normalized dimensionless load is introduced:

$$\beta^+ = \frac{\beta_f - \beta}{\beta_f - \frac{\pi^2}{4}} = \beta\frac{4}{\pi^2}\left(1 + k_p^*\right) - k_p^* \tag{29}$$

The dimensionless length of the plasticized zone, l_0^*, i.e. the l_0/L, ratio is first plotted vs. β in Fig. 3 and finally plotted vs. the normalized load β^+ in Fig. 4. It is shown that the plasticity length, l_0, increases during the yield process which is associated with a decreasing of the dimensionless load β.

Otherwise, it is worth mentioning that the elastic limit case is obtained for:

$$k_p^* \to \infty \Rightarrow \tan\left[\sqrt{\beta}(1 - l_0^*)\right]\tan\left(l_0^*\sqrt{\beta}\right) \to 1 \Rightarrow \beta \to \frac{\pi^2}{4} \tag{30}$$

And the perfect elastoplastic limit case is obtained for: $k_p^* \to 0 \Rightarrow l_0^* \to 0$. It is confirmed that plasticity localizes in a zero-length hinge in case of perfect plasticity constitutive law (i.e. $k_p^* \to 0$).

3.2.4. Load–deflection relationship

The parameters of the general solution of the deflection given in Eq. (21) can be determined as follow for the lower plasticized part, if $x \in [0; l_0[$. The boundary conditions in Eqs. (23-a) and (24-a) lead respectively to:

$$B_1 = \frac{k_p^*}{\beta}B_3 \text{ with } B_3 = \frac{\kappa_y^*}{(1+k_p^*)\cos\left(l_0^*\sqrt{\rho^+}\right)}; \tag{31}$$

The parameters of the general solution of the deflection given in Eq. (22), for the upper part, i.e. for $x \in [l_0, L]$ are determined using boundary conditions in Eqs. (24-b), (25-a) and (24-d) leading respectively to:

$$C_1 = \frac{\kappa_y^*}{\rho^+}\left[\frac{1}{k_p^*} + \frac{1}{\cos\left(l_0^*\sqrt{\rho^+}\right)}\right] \text{ and}$$
$$C_3 = -\tan\left(\sqrt{\beta}\right)C_4 \text{ with}$$
$$C_4 = \frac{\kappa_y^*}{\beta\left[\tan\left(\sqrt{\beta}\right)\cos\left(l_0^*\sqrt{\beta}\right) - \sin\left(l_0^*\sqrt{\beta}\right)\right]} \tag{32}$$

The dimensionless tip deflection, $\delta^* = w^{*+}(1)$, can be finally written:

$$\delta^* = C_1 + C_2 + C_3\cos\sqrt{\beta} + C_4\sin\sqrt{\beta} = C_1 \tag{33}$$

ρ^+, defined in Eq. (19) can be written according to β and β_f, defined in Eq. (28):

$$\rho^+ = \frac{\pi^2}{4}\frac{\beta}{\beta_f} \tag{34}$$

This dimensionless loading factor can be substituted in Eq. (32) to give from Eq. (33) the dimensionless load–tip deflection relationship:

$$\delta^* = \frac{\kappa_Y^*}{\beta\left(1+k_p^*\right)}\left[1 + \frac{k_p^*}{\cos\left(\frac{\pi}{2}l_0^*\sqrt{\frac{\beta}{\beta_f}}\right)}\right] \tag{35}$$

The dimensionless load, β, is plotted according to the dimensionless deflection ratio δ^*/κ_Y^* for various values of k_p^* in Fig. 5. It can be checked that the characteristic elastic point $(\delta^* = 4\kappa_Y^*/\pi^2; \beta = \pi^2/4)$ is solution of Eq. (35).

It is worth to note that if $l_0^* \to 0$ and $k_p^* \to 0$ then $\delta^* \to \kappa_Y^*/\beta$, i.e. there is a continuity with the perfect elastoplastic case, established in Section 3.1 and Eq. (17). On the other hand, if $l_0^* \to 1$ then, as shown in Eq. (28), $\beta \to \beta_f$, and Eq. (35) leads to $\delta^* \to \infty$. This point confirms that the load decreases toward the minimum load capacity of the column at the end of the post-buckling path, β_f. Some asymptotic values in such a case with $k_p^* > 0$, are reported along the ends of some load–deflection curves plotted in Fig. 5, with $k_p^* = 1$; 3; 10 and 30, to illustrate the asymptotic tendency of β.

Moreover, when $k_p^* \to +\infty$, the tangent bending modulus tends toward EI beyond κ_Y^*, i.e. like in the perfect elastic case with no elastic yield curvature. Since only small rotation theory is used in this study, the post-buckling behavior tends to be perfectly elastic and β appears constant, i.e. $\beta = \pi^2/4$, whatever the considered deflection, as demonstrated in Eq. (30) and shown in Fig. 5.

4. Resolution – softening with the gradient plasticity law

4.1. Wood's paradox in case of local softening

It can be shown that the consideration of a local softening elastoplastic bending-curvature law leads to Wood's paradox for the post-buckling problem. In other words, the plasticity zone cannot propagate within a "local" softening law, and a nonlocal plasticity is need to overcome this paradox.

The proof of Wood's paradox in this post-buckling problem can be obtained from the continuity of the plastic curvature along the elastoplastic boundary $x = l_0$:

$$\chi_p(l_0) = 0 \quad \Rightarrow \quad M(l_0) = M_p \tag{36}$$

From the equilibrium equations for the fundamental buckling mode, the gradient of the bending moment is negative, and then the bending moment is a decreasing function with respect to the spatial coordinate:

$$M' = -Pw' \leqslant 0 \quad \Rightarrow \quad M(0) \geqslant M_p \tag{37}$$

However, from the local softening constitutive law, the bending moment is necessarily lower than the yield moment M_p

$$M(x) \leqslant M_p \tag{38}$$

It means that the plasticity length is necessarily vanishing for a local softening plasticity law $l_0 = 0$. In other words, the elastic unloading solution is the only one induced by the "local" character of the constitutive law.

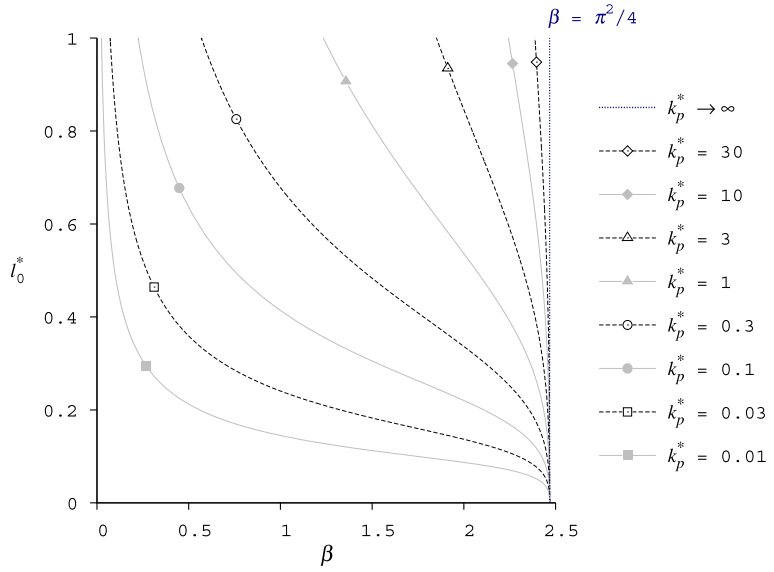

Fig. 3. Propagation of the dimensionless plasticity length, l_0^*, along the column according to the dimensionless load β, for various positive values of k_p^* (local hardening case).

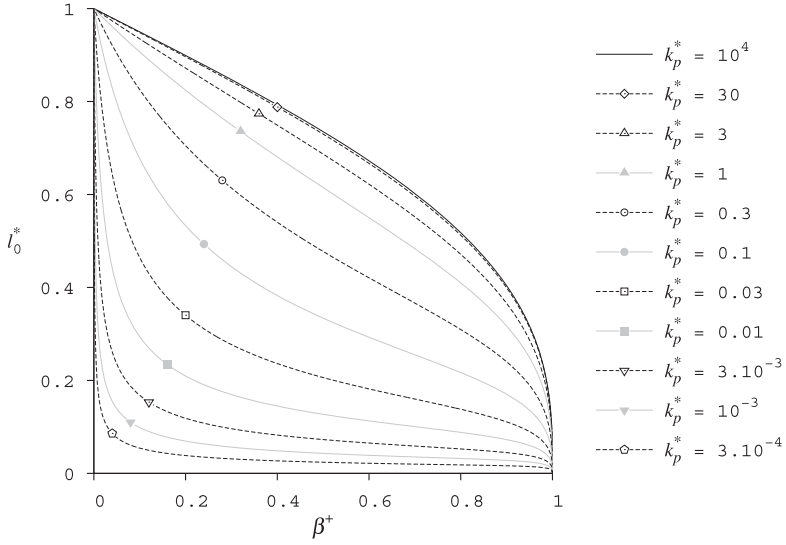

Fig. 4. Propagation of the dimensionless plasticity length, l_0^*, along the column according to the normalized dimensionless load β^+, for various positive values of k_p^* (local hardening case).

4.2. General equation of the deflection

In case of softening behavior at the section scale, $k_p < 0$, the tangent modulus is negative, but the plastic bending modulus has also to satisfy another inequality: $k_p > -EI$ to be physically consistent and avoid any local snap back. As a consequence, the dimensionless plastic modulus defined in Eq. (9) ranges from -1 to 0 in case of softening, i.e. $-1 < k_p^* < 0$.

In the following, the non local softening plasticity constitutive law in Eq. (4) will be considered. In order to solve the fourth-order linear differential equation of the plastic curvature given into Eq. (12), the positive parameter ω is introduced:

$$\omega = \beta + \frac{1}{\alpha^2} - \frac{\lambda_c^2 \beta}{\alpha^2 k_p^*} \tag{39}$$

The Eq. (12) can be now reduced to:

$$\chi_p^{*(4)} + \omega \chi_p^{*''} + \frac{\rho^+}{\alpha^2}\chi_p^* = -\frac{\beta \kappa_Y^*}{\alpha^2 k_p^*} \tag{40}$$

It should be noted that ρ^+ defined in Eq. (20) is negative since $-1 < k_p^* < 0$. If $\alpha > 0$, two additional real parameters ρ_1^- et ρ_2^- respectively positive and negative are introduced to solve the two equivalent second-order differential equations:

$$\rho_1^- = -\frac{\omega}{2} + \sqrt{\frac{\omega^2}{4} - \frac{\rho^+}{\alpha^2}}, \quad \rho_2^- = -\frac{\omega}{2} - \sqrt{\frac{\omega^2}{4} - \frac{\rho^+}{\alpha^2}} \tag{41}$$

The general solution of the plastic curvature differential equation, see Eq. (40), according to the dimensionless coordinate, x^*, depends on four constants D_3, D_4, D_5 and D_6:

$$\chi_p^* = D_3 \cosh\left(x^* \sqrt{\rho_1^-}\right) + D_4 \sinh\left(x^* \sqrt{\rho_1^-}\right) + D_5 \cos\left(x^* \sqrt{-\rho_2^-}\right) + D_6 \sin\left(x^* \sqrt{-\rho_2^-}\right) - \frac{\kappa_Y^*}{1 + k_p^*} \tag{42}$$

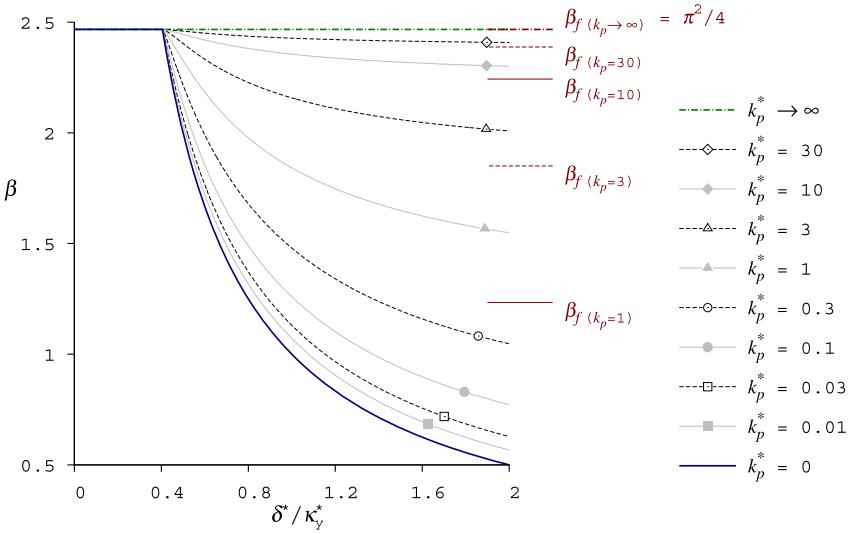

Fig. 5. Dimensionless load, β, according to the normalized tip displacement, δ^*/κ_Y^*, for various positive values of the dimensionless hardening modulus k_p^* (local hardening case).

If $x \in [0; l_0]$, χ_p^* and w^* are related by Eq. (11). The dimensionless deflection named as $w^{-*}(x^*)$ in the first part of the column, where $\chi_p \geqslant 0$, see Fig. 1, depends then on the six constant parameters: D_1–D_6 as follow:

$$w^{-*} = \varphi_1\left[D_3\cosh\left(x^*\sqrt{\rho_1^-}\right) + D_4\sinh\left(x^*\sqrt{\rho_1^-}\right)\right] + \varphi_2\left[D_5\cos\left(x^*\sqrt{-\rho_2^-}\right) + D_6\sin\left(x^*\sqrt{-\rho_2^-}\right)\right] + D_2x^* + D_1 \tag{43}$$

where φ_1 and φ_2 are defined by:

$$\varphi_1 = \frac{\alpha^2 k_p^* \rho_1^- + 1 + k_p^*}{\rho_1^-(1+\lambda_c^2\beta)} \text{ and } \varphi_2 = \frac{\alpha^2 k_p^* \rho_2^- + 1 + k_p^*}{\rho_2^-(1+\lambda_c^2\beta)} \tag{44}$$

Along the upper part of the column, χ_p is vanishing, i.e. $\chi_p = 0$ if $x \in [l_0, L]$, see Fig. 1. The general solution of the dimensionless deflection named as $w^{*+}(x)$ in this elastic zone is similar to the one obtained in Eq. (13), and depends on the four constant parameters: E_1, E_2, E_3, and E_4 as follow:

$$w^{*+} = E_1 + E_2x^* + E_3\cos\left(x^*\sqrt{\beta}\right) + E_4\sin\left(x^*\sqrt{\beta}\right) \tag{45}$$

4.3. Boundary conditions

To solve the deflections of the column in both parts, the eleven following boundary conditions are needed to determine the eleven unknown parameters used in Eqs. (43) and (45): D_1–D_6, B_1–B_4 and l_0.

The nonlocal model introduced in Eq. (4) assumes a nonlocal plastic curvature $\overline{\chi_p}$ based on the Eringen's type of differential equation, initially appearing for nonlocal elasticity, (Eringen, 1983), later used for nonlocal implicit gradient plasticity models by Engelen et al. (2003).

$$\overline{\chi_p} - l_c^2\overline{\chi_p}'' = \chi_p \tag{46}$$

As a consequence, Eq. (4) can be also re-written as follow (see the Appendix A):

$$M = M_p + k_p\left(\overline{\chi_p} + a^2\overline{\chi_p}''\right) = M_p + k_p\left[\left(1+\frac{\alpha^2}{\lambda_c^2}\right)\overline{\chi_p} - \frac{\alpha^2}{\lambda_c^2}\chi_p\right] \tag{47}$$

The two additional boundary conditions (so-called higher-order boundary conditions) in addition to the nine boundary conditions previously presented in Section 3.2.2 valid for a "local" hardening constitutive law, are relative to the derivative of the nonlocal plastic curvature, $\overline{\chi_p}'$ which can be expressed with respect to the higher-order micromorphic plastic moment. Considering the derivative of the local constitutive law presented in Eq. (3) and of the non-locality criteria in Eq. (4), $\overline{\chi_p}'$ can be expressed according to the derivative of plastic curvature χ_p' and the third-order derivative of the deflection, w''', in both cases (see Appendix A). These higher-order boundary conditions can be derived from a variational principle and are valid at the boundaries of the elastoplastic domain, see Eq. (A-12).

- The first higher-order boundary condition in complement to those given in Eq. (23), concerns the clamped section at the bottom of the column ($x = 0$):

$$\overline{\chi_p}'(0) = 0 \Rightarrow \lambda_c^2\left[w^{*+'''}(0) - \chi_p^{*'}(0)\right] + \alpha^2 k_p^*\chi_p^{*'}(0) = 0 \tag{48}$$

- The second additional boundary condition in complement to those given in Eq. (24), is valid at the elastoplastic boundary ($x = l_0$):

$$\overline{\chi_p}'(l_0^*) = 0 \Rightarrow \lambda_c^2\left[w^{*+'''}(l_0^*) - \chi_p^{*'}(l_0^*)\right] + \alpha^2 k_p^*\chi_p^{*'}(l_0^*) = 0 \tag{49}$$

These higher-order boundary conditions can be understood as free micromorphic forces conditions along the boundaries of the elastoplastic domain. Finally, the boundary conditions at the free end of the column are the same than those presented in Eq. (25), in case of hardening constitutive law.

4.4. Propagation of the plasticized zone

The boundary conditions Eqs. (48) lead to $D_2 = D_4 = D_6 = E_2 = 0$. The other boundary conditions lead to the following propagation law of the plasticized zone:

$$\sqrt{\frac{\beta}{\rho_1^-}}\tan\left[\sqrt{\beta}(1-l_0^*)\right]\tanh\left(l_0^*\sqrt{\rho_1^-}\right) = \frac{\frac{\varphi_1}{\varphi_2} - \Lambda\frac{\sqrt{-\rho_2^-}\tanh\left(l_0^*\sqrt{\rho_1^-}\right)}{\sqrt{\rho_1^-}\tan\left(l_0^*\sqrt{-\rho_2^-}\right)}}{\frac{\varphi_1}{\varphi_2} - \Lambda} \tag{50}$$

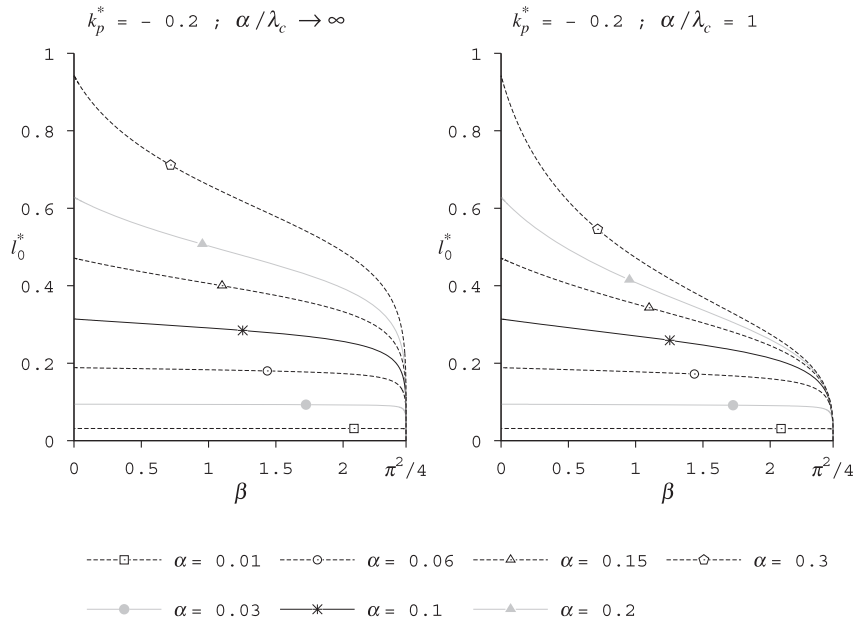

Fig. 6. Propagation of the dimensionless plasticity length, l_0^*, along the column according to the dimensionless load β with $k_p^* = -0.2$ and for various values of α, in case of pure gradient plasticity model and in case of two-scale nonlocal plasticity model with $\alpha/\lambda_c = 1$.

where φ_1 and φ_2 are defined in Eq. (44) and Λ is the following parameter:

$$\Lambda = \frac{\alpha^2\lambda_c^2 k_p^* \rho_1^- + \alpha^2\lambda_c^2\beta k_p^* + \lambda_c^2 k_p^* + \alpha^2 k_p^* - \lambda_c^4\beta}{\alpha^2\lambda_c^2 k_p^* \rho_2^- + \alpha^2\lambda_c^2\beta k_p^* + \lambda_c^2 k_p^* + \alpha^2 k_p^* - \lambda_c^4\beta} \tag{51}$$

It appears that the relationship between l_0^* (or l_0/L ratio), the plasticity localization width, with respect to β, the dimensionless load parameter, does not depend on the yield elastic curvature, (i.e. is independent of κ_Y). It can be checked, using Taylor series on the right side of the Eq. (50), that the following point ($l_0^* = 0$; $\beta = \pi^2/4$), so-called elastic point, is solution, as shown with Eq. (26), since:

$$l_0^* \to 0 \Rightarrow \sqrt{\frac{\beta}{\rho_1^-}}\tan\left[\sqrt{\beta}(1-l_0^*)\right]\tanh\left(l_0^*\sqrt{\rho_1^-}\right) \to 1$$
$$\Rightarrow \quad \cos\left[\sqrt{\beta}(1-l_0^*)\right] \to 0 \Rightarrow \beta \to \frac{\pi^2}{4} \tag{52}$$

The post-buckling elastoplastic process starts at the elastic buckling load, ($\beta = \pi^2/4$ for the clamped-free column) as the length of the plasticity zone is initially vanishing. Then, the plasticity zone grows during the nonlocal softening plastic process.

The function $\beta = f(l_0^*)$ deduced presents a first discontinuity on the right side of the Eq. (50), when l_0 grows, starting from the elastic characteristic point. Since we limit our study to the first

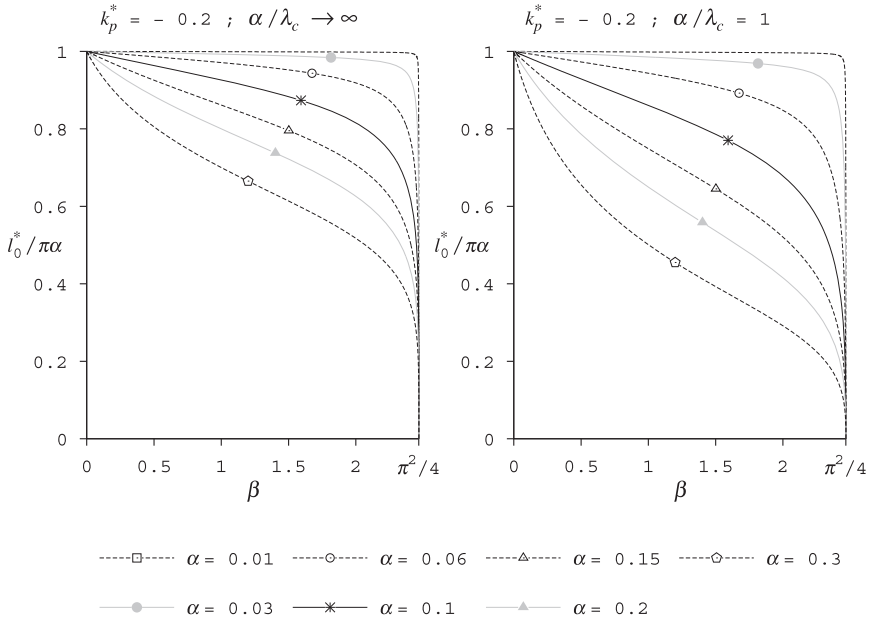

Fig. 7. Propagation of the normalized plasticity length, $l_0^*/\pi\alpha$, along the column according to the dimensionless load β with $k_p^* = -0.2$ and for various values of α, in case of pure gradient plasticity model and in case of two-scale nonlocal plasticity model with $\alpha/\lambda_c = 1$.

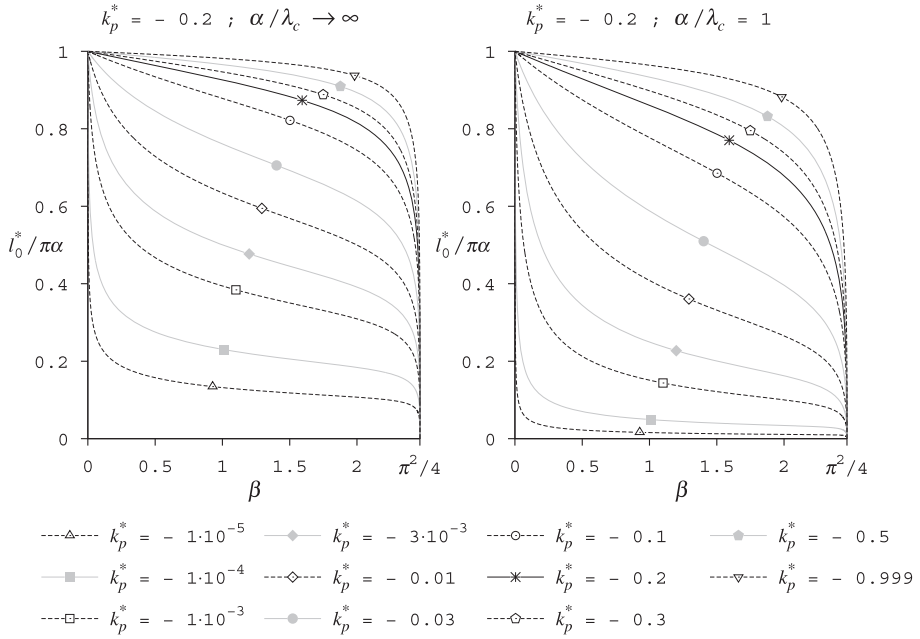

Fig. 8. Propagation of the normalized plasticity length, $l_0^*/\pi\alpha$, along the column according to the dimensionless load β with $\alpha = 0.1$ and for various values of k_p^*, in case of pure gradient plasticity model and in case of two-scale nonlocal plasticity model with $\alpha/\lambda_c = 1$.

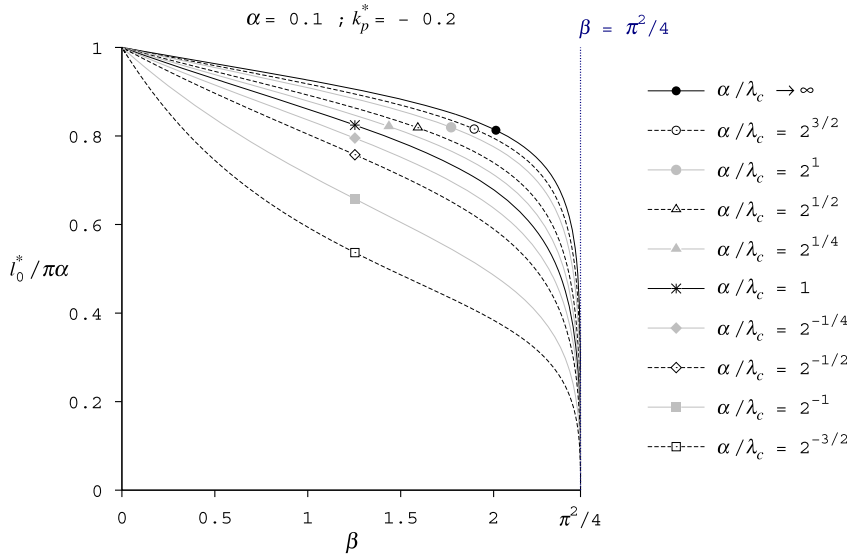

Fig. 9. Propagation of the normalized plasticity length, $l_0^*/\pi\alpha$, along the column according to the dimensionless load β with $\alpha = 0.1$, $k_p^* = -0.2$, and for various values of length scale ratio α/λ_c.

buckling mode, it can be shown that for $l_0^* \in [0; \pi/\sqrt{-\rho_2^-}]$, the function $\beta = f(l_0^*)$ finds a unique solution for β, that ranges in the interval $[\pi^2/4; 0]$. This unique solution can be accurately computed using numerical methods, such as secant method.

In case of pure gradient plasticity model, λ_c is null or $\alpha/\lambda_c \to \infty$. Introducing this assumption in Eq. (51) leads to $\Lambda = 1$. Then, Eq. (50) can be also written directly according to the roots ρ_1^- and ρ_2^- as follow:

$$1 + \sqrt{\frac{\rho_1^-}{\beta}} \tan\left[\sqrt{\beta}(1 - l_0^*)\right] \tanh\left(l_0^* \sqrt{\rho_1^-}\right) = \frac{\rho_2^-(\beta + \rho_1^-)}{\beta(\rho_2^- - \rho_1^-)} \left[1 + \sqrt{\frac{\rho_1^-}{\rho_2^-}} \frac{\tanh\left(l_0^* \sqrt{\rho_1^-}\right)}{\tan\left(l_0^* \sqrt{-\rho_2^-}\right)}\right] \tag{53}$$

It should be noted that pure nonlocal model, i.e. $\alpha = 0$ and $\lambda_c \neq 0$, is not suitable in such problem, since the resolution of Eq. (12) needs $\alpha \neq 0$ if k_p is negative, i.e. in softening cases.

The evolution of plasticity zone of the beam according to the dimensionless load parameter is plotted for various values of α in case of pure gradient plasticity model, i.e. $\alpha/\lambda_c \to \infty$, and in case of two-scale nonlocal plasticity model with $\alpha/\lambda_c = 1$, see Fig. 6.

It is worth to note that the maximum length of the plasticity zone, reached at the end of the post-buckling path, i.e. when $\beta \to 0$, depends only on α. Since, $\rho_2^- \to 1/\alpha^2$, $\rho_1^- \to 0$, and $\varphi_1 \rho_1^- \to 1 + k_p^*$, a multiplication of the numerator and denominator by ρ_1^-/ρ_2^- of the right side of Eq. (50), and a multiplication by $\sqrt{\rho_1^-}$ of both terms lead to:

$$\beta \to 0 \Rightarrow \tan\left(l_0^* \sqrt{-\rho_2^-}\right) \to 0 \Rightarrow l_0^* \to \pi\alpha \tag{54}$$

Thereafter, the propagation of the plasticity zone, l_0^*, is also normalized according to $l_0^*/\pi\alpha$ in order to compare these propagations for various values of α. in Fig. 7. As expected, the plasticity length decreases when α decreases and its propagation is sharper. The columns asymptotically behaves as a column with a local softening law when α is sufficiently small, and presents a more brittle response.

Fig. 8 shows that the plasticity length tends to remain located very closed to the clamped base of the column if $k_p^* \to 0$, in accordance with results obtained in case of perfect plasticity in Section 3.1. Otherwise, it is worth to note that in case of elastic brittle material, for $k_p^* \to -1$, the localization length l_0^* tends to be constant during the softening process and is equal to $\pi\alpha$.

Comparisons within Figs. 6–8 show that the plasticity length tends to increase when the scale ratio, α/λ_c, increases. Fig. 9 confirms this observation with more details. As a consequence, the introduction of the nonlocal length scale λ_c moderates the spreading of the plasticity length.

4.5. Load–deflection relationship

The parameters of the general solution of the deflection given in Eq. (43) can be determined as follow within the plasticity zone, if $x \in [0, l_0[$. The boundary conditions in Eq. (49) and in Eq. (24-a) lead respectively to:

$$D_3 = \frac{\frac{\kappa_Y^*}{1+k_p^*}\frac{1}{\cosh\left(l_0^*\sqrt{\rho_1^-}\right)}}{1+\frac{\Lambda\sqrt{\rho_1^-}}{\sqrt{-\rho_2^-}}\frac{\tanh\left(l_0^*\sqrt{\rho_1^-}\right)}{\tan\left(l_0^*\sqrt{-\rho_2^-}\right)}} \tag{55}$$

and

$$D_5 = \frac{\frac{\kappa_Y^*}{1+k_p^*}\frac{1}{\cos\left(l_0^*\sqrt{-\rho_2^-}\right)}}{1+\frac{\sqrt{-\rho_2^-}}{\Lambda\sqrt{\rho_1^-}}\frac{\tan\left(l_0^*\sqrt{-\rho_2^-}\right)}{\tanh\left(l_0^*\sqrt{\rho_1^-}\right)}} \tag{56}$$

The boundary conditions in Eq. (23-a) gives also:

$$D_1 = -\varphi_1 D_3 - \varphi_2 D_5 \tag{57}$$

The parameters of the general solution of the deflection given in Eq. (45), for the upper part (elasticity zone), if $x \in [l_0, L]$ are determined using boundary conditions Eqs. (25-a) and (24-d) leading respectively to:

$E_3 = -E_4 \tan\sqrt{\beta}$ with

$$E_4 = \frac{D_3\varphi_1\rho_1^-\cosh\left(l_0^*\sqrt{\rho_1^-}\right) + D_5\varphi_2\rho_2^-\cos\left(l_0^*\sqrt{-\rho_2^-}\right)}{\beta\left[\tan(\sqrt{\beta})\cos\left(l_0^*\sqrt{\beta}\right) - \sin\left(l_0^*\sqrt{\beta}\right)\right]} \tag{58}$$

and the boundary conditions Eq. (24-b) finally gives:

$$E_1 = D_3\varphi_1\left[\cosh\left(l_0^*\sqrt{\rho_1^-}\right)\left(1+\frac{\rho_1^-}{\beta}\right) - 1\right] + D_5\varphi_2\left[\cos\left(l_0^*\sqrt{-\rho_2^-}\right)\left(1+\frac{\rho_2^-}{\beta}\right) - 1\right] \tag{59}$$

The dimensionless tip deflection, $\delta^* = w^{*+}(1)$, can be therefore written as follow:

$$\delta^* = E_1 + E_2 + E_3\cos\sqrt{\beta} + E_4\sin\sqrt{\beta} = E_1 \tag{60}$$

and, according to Eq. (59), the dimensionless displacement is finally obtained from:

$$\delta^* = \frac{\kappa_Y^*}{1+k_p^*}\left[\frac{\varphi_1\left(1+\frac{\rho_1^-}{\beta}-\frac{1}{\cosh\left(l_0^*\sqrt{\rho_1^-}\right)}\right)}{1+\frac{\Lambda\sqrt{\rho_1^-}}{\sqrt{-\rho_2^-}}\frac{\tanh\left(l_0^*\sqrt{\rho_1^-}\right)}{\tan\left(l_0^*\sqrt{-\rho_2^-}\right)}} + \frac{\varphi_2\left(1+\frac{\rho_2^-}{\beta}-\frac{1}{\cos\left(l_0^*\sqrt{-\rho_2^-}\right)}\right)}{1+\frac{\sqrt{-\rho_2^-}}{\Lambda\sqrt{\rho_1^-}}\frac{\tan\left(l_0^*\sqrt{-\rho_2^-}\right)}{\tanh\left(l_0^*\sqrt{\rho_1^-}\right)}}\right] \tag{61}$$

The dimensionless tip displacement, depends both on κ_Y^* and β. δ^* can be also normalized with respect to the dimensionless yield curvature δ^*/κ_Y^* for various values of k_p^*, α and λ_c in the next figures (Figs. 10–16).

It can be checked, using Taylor series, that the characteristic elastic point $\left(\delta^* = \frac{4\kappa_Y^*}{\pi^2}; \beta = \frac{\pi^2}{4}\right)$ is solution of Eq. (61) since:

$$l_0^* \to 0 \Rightarrow \delta^* \to \frac{\kappa_Y^*}{\beta} \tag{62}$$

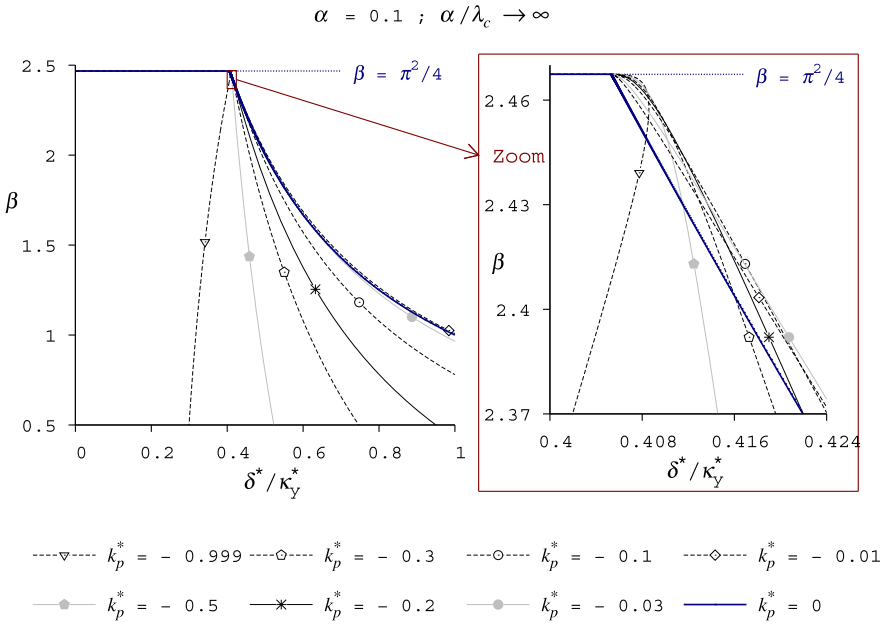

Fig. 10. Dimensionless load, β, according to the normalized tip displacement, δ^*/κ_Y^*, in case of pure gradient plasticity model with $\alpha = 0.1$ and for various negative plastic bending modulus k_p^*.

In case of pure gradient plasticity model ($l_c = 0$), $\alpha/\lambda_c \to \infty$, Eq. (51) leads to $\Lambda = 1$ and Eq. (44) gives:

$$\varphi_1 = \alpha^2 k_p^* + \frac{1+k_p^*}{\rho_1^-} = -\frac{k_p^*}{\beta}\left(1+\alpha^2\rho_1^-\right) \tag{63}$$

and:

$$\varphi_2 = \alpha^2 k_p^* + \frac{1+k_p^*}{\rho_2^-} = -\frac{k_p^*}{\beta}\left(1+\alpha^2\rho_2^-\right) \tag{64}$$

Introducing Eqs. (63) and (64) into Eq. (62), the dimensionless tip displacement in case of pure gradient plasticity model ($l_c = 0$), can be then written directly according to the roots ρ_1^- and ρ_2^- as follow:

$$\delta^* = \frac{\kappa_Y^* k_p^*}{\beta\left(1+k_p^*\right)}\left[\begin{array}{l}\left(1+\alpha^2\rho_1^-\right)\dfrac{\dfrac{1}{\cosh\left(l_0^*\sqrt{\rho_1^-}\right)}^{-\frac{\rho_1^-}{\beta}}-1}{1+\dfrac{\sqrt{\rho_1^-}\tanh\left(l_0^*\sqrt{\rho_1^-}\right)}{\sqrt{-\rho_2^-}\tan\left(l_0^*\sqrt{-\rho_2^-}\right)}} \\ +\left(1+\alpha^2\rho_2^-\right)\dfrac{\dfrac{1}{\cos\left(l_0^*\sqrt{-\rho_2^-}\right)}^{-\frac{\rho_2^-}{\beta}}-1}{1+\dfrac{\sqrt{-\rho_2^-}\tan\left(l_0^*\sqrt{-\rho_2^-}\right)}{\sqrt{\rho_1^-}\tanh\left(l_0^*\sqrt{\rho_1^-}\right)}}\end{array}\right] \tag{65}$$

This relationship has been previously demonstrated in another way in case of pure gradient plasticity model by Picandet et al. (2013). As previously observed in case of positive hardening

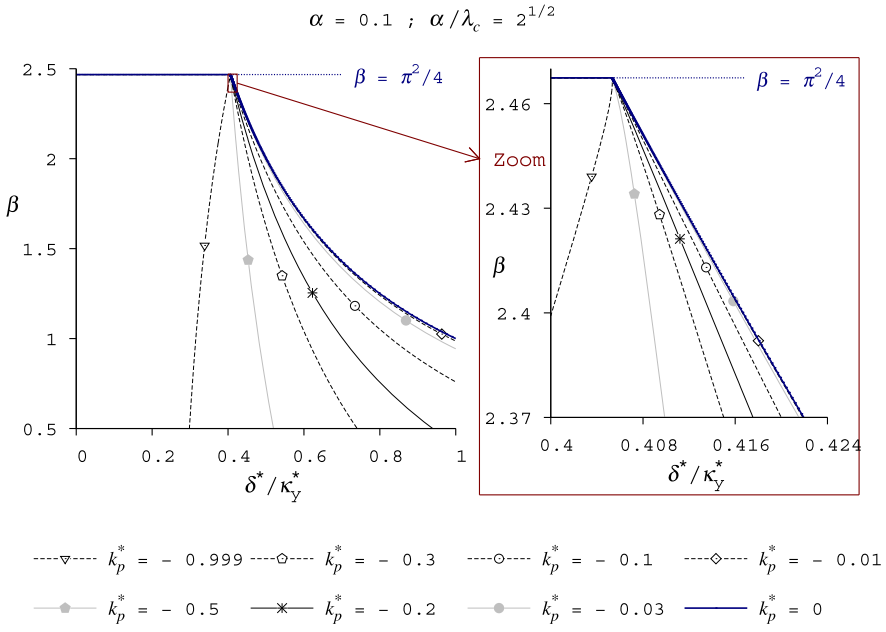

Fig. 11. Dimensionless load, β, according to the normalized tip displacement, δ^*/κ_Y^*, with $\alpha = 0.1$, $\alpha/\lambda_c = 2^{1/2}$ and for various negative plastic bending modulus k_p^*.

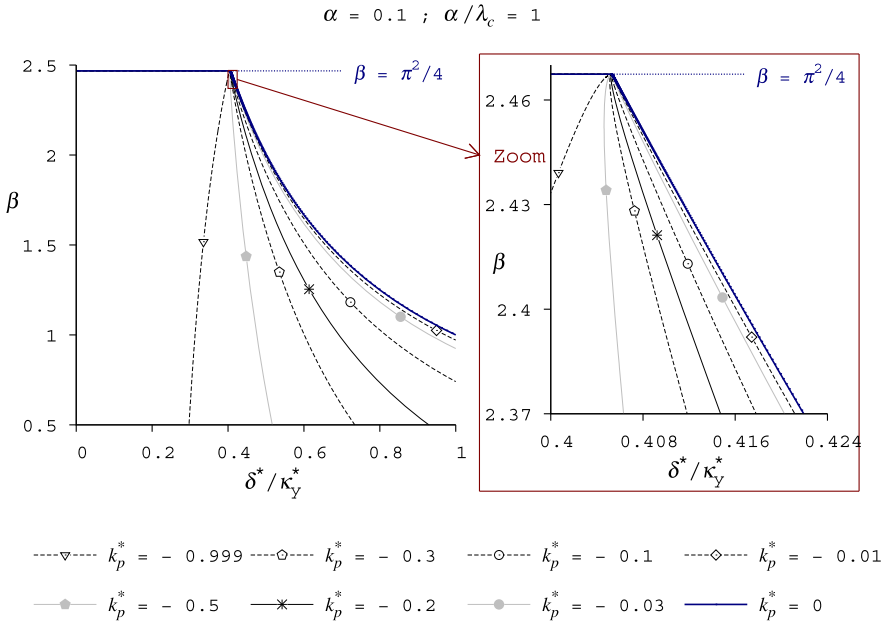

Fig. 12. Dimensionless load, β, according to the normalized tip displacement, δ^*/κ_Y^*, with $\alpha = 0.1$, $\alpha/\lambda_c = 1$ and for various negative plastic bending modulus k_p^*.

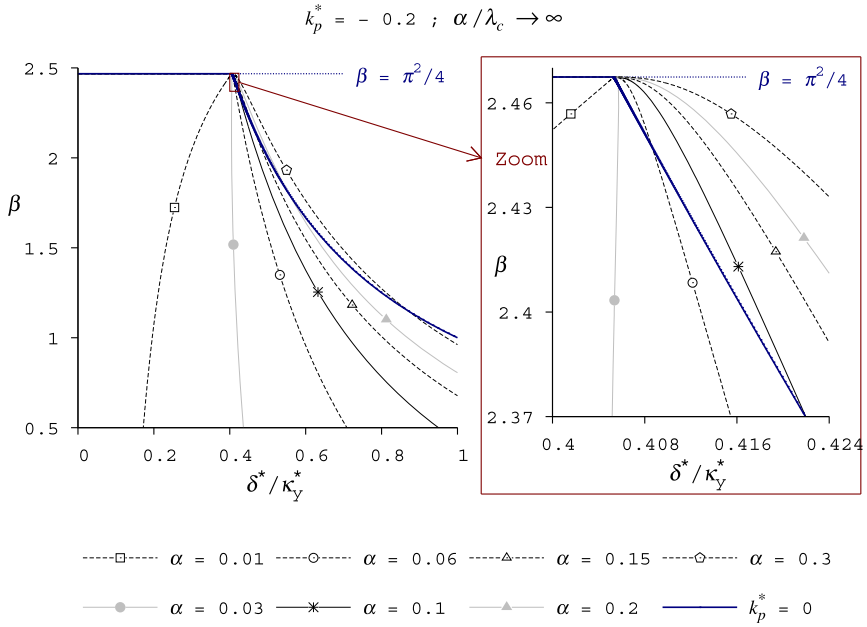

Fig. 13. Dimensionless load, β, according to the normalized tip displacement, δ^*/κ_Y^*, in case of pure gradient plasticity model with $k_p^* = -0.2$ and for various values of α.

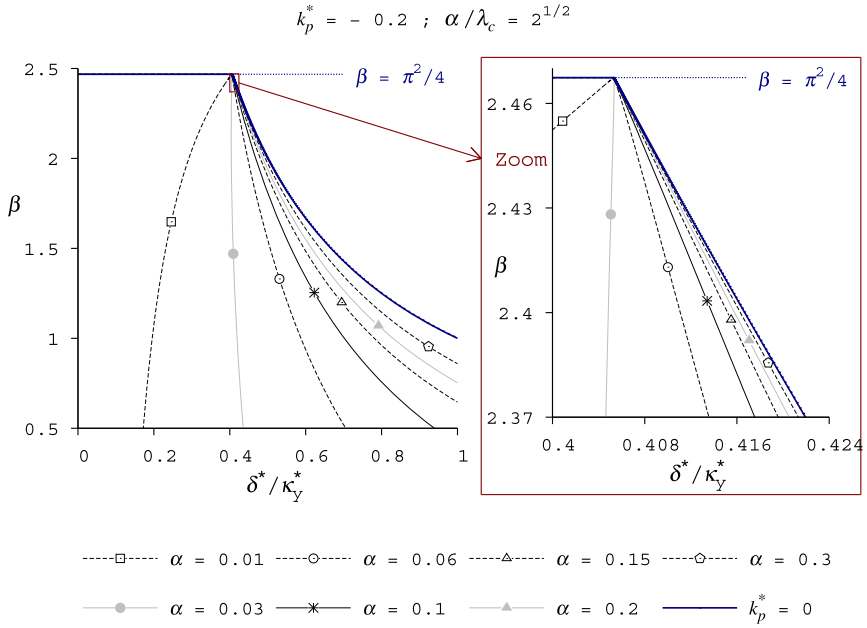

Fig. 14. Dimensionless load, β, according to the normalized tip displacement, δ^*/κ_Y^*, with $k_p^* = -0.2$, $\alpha/\lambda_c = 2^{1/2}$ and for various values of α.

(cf. Section 3.2.4), δ^* is relative to κ_Y^* and the normalized dimensionless displacement δ^*/κ_Y^* is considered to study the dimensionless load–tip deflection relationship.

4.6. Parametric study

Dimensionless tip displacements plotted in Figs. 10–16 present the general post-buckling path with various parameters such as length scale ratios α/λ_c, the plastic bending modulus k_p^* and the gradient plasticity parameter α. Focus on the beginning of the post buckling path close to the elastic point with the same parameters is also shown in each figure while the perfect elastoplastic case, i.e. $k_p^* = 0$ and $\alpha = \lambda_c = 0$, is always plotted as reference, see Section 3.1.

The dimensionless tip displacement in case of pure gradient plasticity model, i.e. $\alpha/\lambda_c \to \infty$, is first plotted for various values of k_p^* and α, in Fig. 10 and in Fig. 13 respectively. The tip displacements, in case of two-scale nonlocal plasticity are also consecutively plotted with two length scale ratios: $\alpha/\lambda_c = \sqrt{2}$, in Figs. 11 and 14, and $\alpha/\lambda_c = 1$, in Figs. 12 and 15.

To compare the influence of the plastic bending modulus, k_p^* and of the gradient plasticity parameter, α, with a given length scale ratio, the reference setting values of each dimensionless parameter are fixed to a constant values: $k_p^* = -0.2$ and $\alpha = 0.1$. These reference values are considered as representative of many engineering cases, such as the buckling of usually designed column of reinforced concrete.

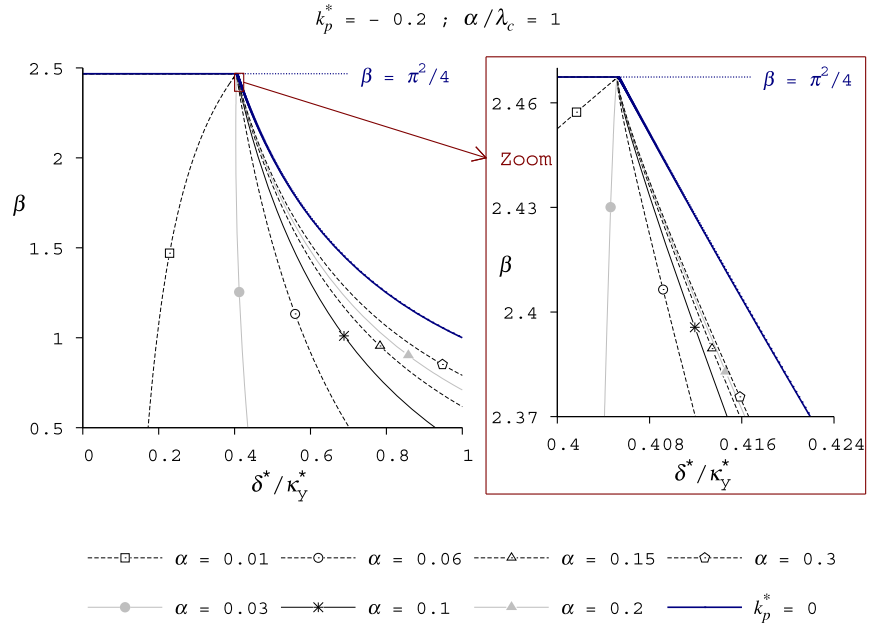

Fig. 15. Dimensionless load, β, according to the normalized tip displacement, δ^*/κ_Y^*, with $k_p^* = -0.2$, $\alpha/\lambda_c = 1$ and for various values of α (nonlocal softening case).

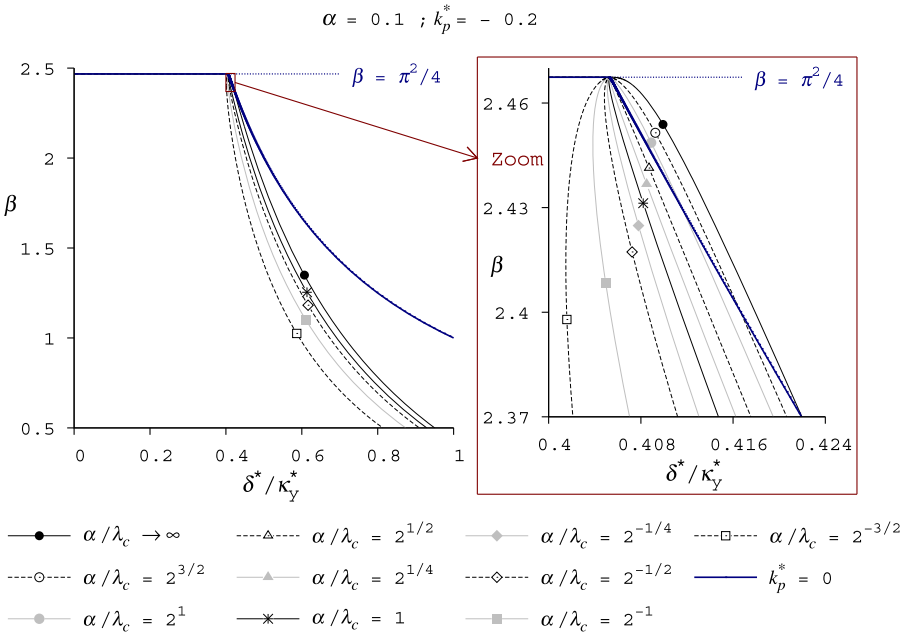

Fig. 16. Dimensionless load, β, according to the normalized tip displacement, δ^*/κ_Y^*, with $\alpha = 0.1$, $k_p^* = -0.2$, and for various values of length scale ratio α/λ_c.

4.6.1. Influence of the plastic bending modulus, k_p^*

Figs. 10–12 show that the global load–deflection relationship deviates gradually from the perfect elastoplastic case when k_p^* decreases toward -1, especially when $\alpha/\lambda_c < \sqrt{2}$ and $\beta < 1.5$.

Close to the elastic point, whatever the length scale ratio, a greater deviation of the post buckling path from the perfect elastoplastic case is observed when k_p^* decreases toward -1. On the opposite boundary, the figures illustrate the continuity of the load–deflection relationship according to k_p^* since the global post buckling paths tend always toward the perfect elastoplastic behavior when $k_p^* \to 0$.

4.6.2. Influence of the length scales

Figs. 13–15 show that increasing length scales reduce the snap back of the global load–deflection relationship, especially with the highest length scale ratios, i.e. when the gradient model is dominant. In particular, if $\alpha/\lambda_c < \sqrt{2}$, α has a significant influence on the beginning of the post buckling path. Actually, the decrease of k_p^* magnifies the effect of an initiation of the length scale and vice versa.

4.6.3. Influence of characteristic length scale ratios α/λ_c

It is numerically observed a snap back, appearing at the beginning of the post buckling path if $\alpha/\lambda_c < \sqrt{2}$, while a slight hardening

behavior is observed if $\alpha/\lambda_c < \sqrt{2}$ since the dimensionless load parameter is surprisingly above the perfect elastoplastic case. Introduction of the second length scale, λ_c, allow to regulate this apparent hardening effect, also observed in Challamel et al. (2008), which is probably induced by the gradient plasticity model on the load–deflection relationship. Moreover, numerical results show that the load–deflection relationship tends asymptotically toward those of the perfect elastoplastic case if $\alpha/\lambda_c = \sqrt{2}$. In another way, the initial snap back is magnified when the integral nonlocal model becomes dominant, i.e. with the lowest length scale ratio α/λ_c.

These observations can be noticed in the previous figures showing a closer look of the beginning of the post buckling. A more closer look would be however needed to make the same deduction with the highest values of k_p^*. The effect of the length scale ratio on the global post buckling path and on its initiation are shown in Fig. 16 with more details.

Generally, the length scale ratio has a moderate effect on the global load–deflection relationship but has a significant effect close to the elastic point. Therefore, the introduction of the second length scale, λ_c, allows to efficiently regulate the theoretical initialization of the post buckling path according to the internal characteristics of the material.

5. Conclusion

In this paper, the behavior of an axially loaded elastoplastic column is studied within a simple elastoplastic moment–curvature constitutive law. The applications of such a study can be found in various structural engineering problems, including reinforced concrete, steel, timber or composite structures. The post-buckling is studied for a local or a nonlocal linearly hardening or softening plasticity law postulated at the section scale. Linear differential equations are obtained for a second-order analysis coupled to a linearly hardening or softening elastoplastic laws. It is analytically shown that for all kinds of elastoplastic behaviors, hardening, perfectly plastic or nonlocal softening plasticity laws, the plasticity phenomena lead to the global softening phenomenon in the load–deflection diagram (a decrease of the load once the plasticity phenomena are reached). The propagation of the plasticity zone during the post-buckling process is analytically characterized both for the hardening or the softening plasticity laws.

As usually observed in case of local softening constitutive laws, it is shown that the unphysical elastic unloading solution necessarily occurs in presence of local softening moment–curvature constitutive law (also called Wood's paradox). A nonlocal plasticity moment–curvature softening law is then incorporated to control the localization branch in the post-buckling stage. This nonlocal plasticity model is a two-scale nonlocal plasticity model that can be cast in a micromorphic framework. This nonlocal plasticity law includes for instance the explicit gradient plasticity law. Higher-order plasticity boundary conditions are derived from an extended variational principle. Some parametric studies finally illustrate the interest and the main findings of the methodology. They confirm the continuity of the presented model according to the plastic bending modulus of the column, i.e. between the linear hardening and softening plasticity laws. Such model strongly depends on the characteristic length of the macroscopic nonlocal constitutive laws. These cross-sectional dependent characteristic lengths of the nonlocal bending-curvature elastoplastic model are typically macroscopic phenomenological parameters, that still merit further calibration studies from the two-dimensional cross-section failure mechanism.

Nomenclature

	Parameters	Dimension	Corresponding dimensionless parameters
a	characteristic length (gradient plasticity parameter)	[L]	$\alpha = a/L$
E	young modulus	$[M.L^{-1}.T^{-2}]$	–
I	area moment of inertia	$[L^4]$	–
k_p	plastic bending modulus	$[M.L^3.T^{-2}]$	$k_p^* = k_p/EI$
L	length of the column	[L]	–
l_0	length of the plasticized zone	[L]	$l_0^* = l_0/L$
l_c	characteristic length (nonlocal plasticity parameter)	[L]	$\lambda_c = l_c/L$
M_p	yield moment ($M_P = EI\kappa y$)	$[M.L^2.T^{-2}]$	$\kappa_y^* = M_pL/EI$
P	axial load	$[M.L.T^{-2}]$	$\beta = PL^2/EI$
x	longitudinal coordinate	[L]	$x^* = x/L$
$w(x)$	deflection of the column at x	[L]	$w^* = w/L$
β_f	final post-buckling load	–	see Eq. (28)
δ	tip deflection (free end)	[L]	$\delta^* = w(L)/L = w^*$
χ	total curvature of the column	$[L^{-1}]$	$\chi^* = \chi L$
χ_p	plastic curvature of the column	$[L^{-1}]$	$\chi_p^* = \chi_p L$
$\overline{\chi_p}$	nonlocal plastic curvature	$[L^{-1}]$	see Eq. (46)
κ_y	yield curvature	$[L^{-1}]$	$\kappa_Y^* = \kappa_Y L$
Λ		–	see Eq. (51)
ρ^+	root with $k_p > 0$ see Eq. (20)	–	$\rho^+ = \beta(1 + 1/k_p^*)$
ρ_1^-	positive root with $k_p < 0$ see Eq. (41)	–	$\rho_1^- = -\omega/2 + \sqrt{(\omega^2/4) - (\rho^+/\lambda_c^2)}$
ρ_2^-	Negative root with $k_p < 0$ see Eq. (41)	–	$\rho_2^- = -\omega/2 - \sqrt{(\omega^2/4) - (\rho^+/\lambda_c^2)}$
φ_1			see Eq. (44)
φ_2			see Eq. (44)
ω			see Eq. (39)
ζ	dimensionless parameter of the softening evolution law	–	see Eq. (A-1) or Eq. (A-11)

Appendix A

The aim of this part is to derive variationally-based boundary conditions associated with the implementation of the higher-order plasticity model. Following a variational procedure, the natural and essential boundary conditions of the axially loaded elastoplastic column will be deduced. We start from an elastoplastic energy functional extended to nonlocal plasticity by Challamel et al. (2010), and inspired by the micromorphic

approach developed for elastic and inelastic media, in a consistent thermodynamic framework (Forest, 2009). A similar variational methodology was also presented by Challamel et al. (2008) with an equivalent energy functional. The following energy functional can be chosen for the buckling problem investigated in the paper:

$$W\left[w,\chi_p,\overline{\chi_p}\right]=\int_0^L \frac{1}{2}EI\left(w''-\chi_p\right)^2-P\frac{w'^2}{2}+M_p\chi_p+\frac{k_p}{2}\chi_p^2 +\frac{k_p}{2}(\zeta-1)\left(\chi_p-\overline{\chi_p}\right)^2+\frac{k_p}{2}l_c^2(\zeta-1)\left(\overline{\chi_p}'\right)^2dx \quad \text{(A-1)}$$

where ζ is a dimensionless parameter that appears in the hardening/softening evolution law. The extended energy functional depends on two additional nonlocal parameters, namely the characteristic length, l_c, and the dimensionless parameter, ζ. These two parameters can be equivalently expressed with respect to the two nonlocal length scales, l_c, and a. $W[w,\chi_p,\overline{\chi_p}]$ depends on the deflection $w(x)$, the plastic curvature $\chi_p(x)$ and the nonlocal plastic curvature $\overline{\chi_p}(x)$, the last one can be understood here as an independent variable. Following a classical procedure also used for explicit gradient plasticity models (see Mühlhaus and Aifantis (1991) or de Borst and Mühlhaus (1992)), the overall domain can be divided into a plastic domain and an elastic one.

The first variation of this functional leads to the extremal condition:

$$\delta W\left[w,\chi_p,\overline{\chi_p}\right]=0,\quad \forall\left(\delta w,\delta\chi_p,\delta\overline{\chi_p}\right) \quad \text{(A-2)}$$

This stationarity principle implicitly assumes the loading condition in the plasticity domain. This assumption is valid for monotonic loading with increasing plasticity domain. Otherwise, the loading/unloading conditions should be obtained from application of a variational inequality principle, as shown for instance by Nguyen (2000) for general elastoplastic evolutions (see also Duvaut and Lions (1972) and the recent discussion in Jirásek et al. (2013)).

$$\begin{aligned}\delta W\left[w,\chi_p,\overline{\chi_p}\right]=&\int_0^L EI\left(w''-\chi_p\right)\delta w''-Pw'\delta w'dx\\&+\int_0^{l_0}-EI\left(w''-\chi_p\right)\delta\chi_p+M_p\delta\chi_p\\&+k_p\left(\zeta\chi_p+(1-\zeta)\overline{\chi_p}\right)\delta\chi_p dx-k_p(\zeta-1)\\&\times\int_0^{l_0}\left(\chi_p-\overline{\chi_p}+l_c^2\overline{\chi_p}''\right)\delta\overline{\chi_p}\\&+\frac{k_p}{2}l_c^2(\zeta-1)\left[\overline{\chi_p}'\delta\overline{\chi_p}\right]_0^{l_0}=0\end{aligned} \quad \text{(A-3)}$$

If the nonlocal plastic curvature $\overline{\chi_p}$ is considered as an independent variable, the variational equality valid whatever $\overline{\chi_p}$ leads to the coupled differential equation:

$$\overline{\chi_p}-l_c^2\overline{\chi_p}''=\chi_p \quad \text{(A-4)}$$

It is no more ambiguous that $\overline{\chi_p}$ has the meaning of a nonlocal plastic curvature, the spatial nonlocality being related to the Green's operator associated with the differential equation. Therefore, the first variation of the energy functional can be also simplified as:

$$\delta W[w,\chi_p]=\int_0^L M\delta w''-Pw'\delta w'dx-\int_0^{l_0}M-\left(M_p+M^*\right)\delta\chi_p dx +\frac{k_p}{2}l_c^2(\zeta-1)\left[\overline{\chi_p}'\delta\overline{\chi_p}\right]_0^{l_0}=0 \quad \text{(A-5)}$$

with the associated constitutive law for the elastic bending moment–curvature relationship, and the nonlocal hardening/softening law:

$$M=EI\left(w''-\chi_p\right)\ \text{and}\ M^*=k_p\left(\zeta\chi_p+(1-\zeta)\overline{\chi_p}\right) \quad \text{(A-6)}$$

The extremal condition leads to the equilibrium equation and the yield function:

$$M''+Pw''=0\ \text{and}\ M=M_p+M^* \quad \text{(A-7)}$$

with the variationally-based boundary conditions:

$$\begin{aligned}&M(L)=0,\quad M'(L)+Pw'(L)=0,\quad w(0)=w'(0)=0\\&\overline{\chi_p}'(0)=\overline{\chi_p}'(l_0)=\chi_p(l_0)=0\end{aligned} \quad \text{(A-8)}$$

The high-order boundary conditions of the nonlocal plasticity model are included in these equations, and are applied at the boundary of the elastoplastic domain.

The nonlocal plastic constitutive law appearing from the variational principle is based on a combination of the local plastic curvature and the nonlocal plastic curvature.

$$M^*=k_p\tilde{\chi}_p\ \text{with}\ \tilde{\chi}_p=\zeta\chi_p+(1-\zeta)\overline{\chi_p}=\overline{\chi_p}-\zeta l_c^2\overline{\chi_p}'' \quad \text{(A-9)}$$

Such a combination of local and nonlocal plastic variables was initially proposed by Vermeer and Brinkgreve (1994) for softening evolutions with a stress–strain three dimensional approach (see also Jirásek and Rolshoven (2003)). In the present case, this model can be also written in a differential format (see also Challamel et al. (2008) and Challamel et al. (2010)):

$$M^*-l_c^2M^{*''}=k_p\left[\chi_p-\zeta l_c^2\chi_p''\right] \quad \text{(A-10)}$$

This model can be also referred as an implicit gradient plasticity model (see for instance Engelen et al. (2003)). For a softening evolution, it has been shown by Challamel (2008) that the dimensionless factor ζ should be negative:

$$M^*-l_c^2M^{*''}=k_p\left[\chi_p+a^2\chi_p''\right]\ \text{with}\ \zeta=-\frac{a^2}{l_c^2}\leqslant 0 \quad \text{(A-11)}$$

Even if efficient from the localization properties, such a definition of the regularization factor leads to a non definite positive total energy functional introduced in Eq. (A-1).

Furthermore, it can be shown from the higher-order boundary conditions that:

$$\overline{\chi_p}'=0\quad\Rightarrow\quad M'-k_p\zeta\chi_p'=EI(w'''-\chi_p')+k_p\frac{a^2}{l_c^2}\chi_p'=0 \quad \text{(A-12)}$$

Hence, the higher-order boundary conditions can be expressed with respect to the local variables namely the deflection and the plastic curvature.

References

Aifantis, E.C., 2011. On the gradient approach – Relation to Eringen's nonlocal theory. Int. J. Eng. Sci. 49 (12), 1367–1377.

Bažant, Z.P., 1976. Instability, ductility and size effect in strain-softening concrete. J. Eng. Mech. ASCE 102, 331–334.

Bažant, Z.P., Cedolin, L., 2003. Stability of Structures: Elastic, Inelastic, Fracture, and Damage Theories. Dover Publications.

Calladine, C.R., 1982. Plastic buckling of tubes in pure bending. In: The Building of Structures in Theory and Practice: IUTAM Symposium, pp. 111–124.

Casandjian, C., Challamel, N., Lanos, C., Hellesland, J., 2013. Reinforced Concrete Beams, Columns and Frames: Mechanics and Design. ISTE, John Wiley & Sons.

Challamel, N., 2003. Une approche de plasticité au gradient en construction métallique. C. R. Acad. Sci. 331 (9), 647–654.

Challamel, N., 2008. A regularization study of some softening beam problems with an implicit gradient plasticity model. J. Eng. Math. 62, 373–387.

Challamel, N., 2009. An application of large displacement limit analysis to frame structures. Struct. Eng. Mech. 33, 159–177.

Challamel, N., Hellesland, J., 2013. Buckling of softening columns in a continuum damage mechanics perspective – local versus non-local formulation. Eur. J. Mech. A/Solids 39, 229–242.
Challamel, N., Lanos, C., Casandjian, C., 2008. Plastic failure of nonlocal beams. Phys. Rev. E 78, 026604.
Challamel, N., Lanos, C., Casandjian, C., 2010. On the propagation of localization in the plasticity collapse of hardening–softening beams. Int. J. Eng. Sci. 48 (5), 487–506.
de Borst, R., Mühlhaus, H.B., 1992. Gradient-dependent plasticity: formulation and algorithmic aspects. Int. J. Numer. Methods Eng. 35, 521–539.
Duvaut, G., Lions, J.L., 1972. Les inéquations en mécanique et en physique. Dunod, Paris.
Engelen, R.A.B., Geers, M.G.D., Baaijens, F.P.T., 2003. Nonlocal implicit gradient-enhanced elasto-plasticity for the modelling of softening behaviour. Int. J. Plast. 19, 403–433.
Eringen, A.C., 1983. On differential equations of nonlocal elasticity and solutions of screw dislocation and surface waves. J. Appl. Phys. 54, 4703–4710.
Forest, S., 2009. Micromorphic approach for gradient elasticity, viscoplasticity, and damage. J. Eng. Mech. 135 (3), 117–131.
Hellesland, J., Challamel, N., Casandjian, C., Lanos, C., 2013. Reinforced Concrete Beams, Columns and Frames: Section and Slender Member Analysis. ISTE, John Wiley & Sons.
Jirásek, M., Bažant, Z.P., 2002. Inelastic Analysis of Structures. John Wiley & Sons, ed.
Jirásek, M., Rolshoven, S., 2003. Comparison of integral-type nonlocal plasticity models for strain-softening materials. Int. J. Eng. Sci. 41, 1553–1602.
Jirásek, M., Rokoš, O., Zeman, J., 2013. Localization analysis of variationally based gradient plasticity model. Int. J. Solids Struct. 50, 256–269.
Kyriakides, S., Ju, G.T., 1992. Bifurcation and localization instabilities in cylindrical shells under bending—I. Experiments. Int. J. Solids Struct. 29, 1117–1142.
Kyriakides, S., Ok, A., Corona, E., 2008. Localization and propagation of curvature under pure bending in steel tubes with Lüders bands. Int. J. Solids Struct. 45, 3074–3087.
Mazzolani, F.M., Gioncu, V., 2002. Ductility of Seismic-Resistant Steel Structures. Spon Press.
Mühlhaus, H.B., Aifantis, E.C., 1991. A variational principle for gradient plasticity. Int. J. Solids Struct. 28, 845–857.
Nguyen, Q.S., 2000. Stabilité et mécanique non-linéaire, Hermes.
Peerlings, R.H.J., 2007. On the role of moving elastic–plastic boundaries in strain gradient plasticity. Model. Simul. Mater. Sci. Eng. 15, 109–120.
Picandet, V., Challamel, N., Hin, S., 2013. Comportement au flambement de poteaux avec loi de plasticité au gradient. In: 21ème Congrès Français de Mécanique, Bordeaux.
Pijaudier-Cabot, G., Bažant, Z.P., 1987. Nonlocal damage theory. J. Eng. Mech. 113, 1512–1533.
Polizzotto, C., 2007. Strain-gradient elastic–plastic material models and assessment of the higher order boundary conditions. Eur. J. Mech. A/Solids 26, 189–211.
Poonaya, S., Teeboonma, U., Thinvongpituk, C., 2009. Plastic collapse analysis of thin-walled circular tubes subjected to bending. Thin Walled Struct. 47, 637–645.
Reid, S.R., Yuy, T.X., Yangz, J.L., 1998. An elastic–plastic hardening–softening cantilever beam subjected to a force pulse at its tip: a model for pipe whip. Proc. R. Soc. Lond. A 454, 997–1029.
Vaz, M.A., Patel, M.H., 2007. Post-buckling behaviour of slender structures with a bi-linear bending moment–curvature relationship. Int. J. Non-linear Mech. 42, 470–483.
Vermeer, P.A., Brinkgreve, R.B.J., 1994. A new effective non-local strain measure for softening plasticity. In: Chambon, R., Desrues, J., Vardoulakis, I. (Eds.), Rotterdam, Balkema, 1994, pp. 89–100.
Wood, R.H., 1968. Some controversial and curious developments in the plastic theory of structures. In: Heyman, J., Leckie, F.A. (Eds.), Engineering Plasticity. Cambridge University Press, UK.
Yu, T.X., Reid, S.R., Wang, B., 1993. Hardening–softening behaviour of tubular cantilever beams. Int. J. Mech. Sci. 35, 1021–1033.